Tech Science Press

Biocomposite Films of Polylactic Acid Reinforced with Microcrystalline Cellulose from Pineapple Leaf Fibers

Galia Moreno, Karla Ramirez, Marianelly Esquivel and Guillermo Jimenez*

Laboratory of Polymers (POLIUNA), School of Chemistry, Universidad Nacional, Heredia, Costa Rica.

*Corresponding Author: Guillermo Jimenez. Email: gjime@una.cr.

Abstract: Poly(lactic acid) (PLA) composite films reinforced with microcrystalline cellulose (MCC) extracted from pineapple leaf fibers (PALF) were prepared by a solution casting procedure. In an attempt to improve the interaction between PLA and cellulose, two approaches were adopted; first, poly(ethylene glycol) (PEG) was used as a surfactant, and second, the cellulosic fibers were pre-treated using *tert*-butanol (TBA). Lignocellulosic and cellulosic substrates were characterized using Fourier transform infrared (FTIR), wide-angle X-ray scattering (WAXS), and thermogravimetrical analysis (TGA). MCC from PALF showed good thermal stability, left few residues after decomposing, and exhibited high crystallinity index. Mechanical, thermal and thermomechanical properties of the PLA composites were also evaluated. Multiple PLA endotherms were observed in composites with TBA-treated MCC due to crystal nucleation effects. The ultimate tensile strain values for all composites were lower than that of the pristine PLA. However, 4 wt. % MCC content provided balanced engineering properties in terms of static and dynamic tensile properties.

Keywords: Cellulose; composites; microcrystalline; PLA; pineapple

1 Introduction

Microcrystalline cellulose (MCC) is the particulate form of cellulose and has been employed as filler and agglutinant [1]. MCC is prepared by hydrolysis of native α-cellulose, commercially obtained from wood and cotton. It has been known that MCC properties might vary according to the crystallinity, humidity content, surface area, porosity, and molecular weight of the cellulosic source [1]. A number of cellulosic sources have also been explored in the last twenty years such as bagasse [2,3], flax and hemp [4,5], soybean [6] and pineapple [7], among others. Pineapple (*Ananas comosus*) is a major export product in Costa Rica with an annual volume of 2.5 million metric tons according to statistics of the Food and Agricultural Organization (FAO). Pineapple industrialization in Costa Rica yields approximately 1.5 million metric tons of pineapple leafs fibers (PALF) as a by-product. The annual sheer volume of PALF combined with its natural slow rate of biodegradation poses major environmental challenges. Almost half of the Costa Rican PALF is made of alpha-cellulose (45 wt. %) with lignin as the second major component (28 wt. %) [8]. This high alpha-cellulose content makes PALF a remarkably abundant source for cellulose, MCC, cellulose derivatives and nanocellulose, among other products.

Lignocellulosic materials have been lately drawing attention as filler and reinforcing components for biodegradable polymeric composites [9]. One of the biodegradable polymer matrices for polymer/MCC composites that have been studied is poly (lactic acid), PLA [10-15]. Vast majority of earlier studies on MCC has been based on wood sources, and only few of them were focused on pineapple by-products such as PALF [14].

One of the main drawbacks of PLA resin is its poor thermal resistance that can be overcome either by performing stereocomplexation of both enantiomeric forms of PLA, poly (L-lactic acid), PLLA, and poly (D-lactic acid), PDLA [15] or by adding reinforcing materials such as nanoclay [16]. Both scenarios imply a more costly PLA, turning it into a less competitive plastic against commercial polyolefins used in

DOI: 10.32604/jrm.2019.00017

disposable glassware, grocery bags, etc. An alternative to this issue is to use green fillers such as MCC which has been reported to increase PLA thermal stability [10,11,14,17]. Furthermore, PLA is a brittle polymer, and this property can be worsened upon the addition of the filler. This effect can be reduced by using surfactants such as low-molecular weight polyethylene glycol (PEG) [18,19].

In this work, PLA/MCC biocomposite films were prepared using PALF as a source of MCC. In order to improve the interaction of MCC with the polymer matrix, a pre-treatment of the cellulosic fibers with *tert*-butanol (TBA) was also carried out, using (PEG) as a surfactant agent.

2 Materials and Methods

2.1 Materials

PLA (Ingeo, 7000D bottle grade from Nature Works, Minnetonka, MN, USA) was kindly supplied by Cosalco Co. (Costa Rica), and PALF was collected at Inprotsa Farm (northern Costa Rica) which produces MD2 pineapple. Fisher Scientific Carbowax 400 PEG, and TBA were used as surfactant and presoaking treatment of the MCC, respectively. Common chemical reagents such as hydrochloric acid, sodium hydroxide, ammonium, and sodium chlorite were used to bleach and extract MCC from PALF.

2.2 Microcrystalline Cellulose Preparation and Characterization

Handling of the lignocellulosic substrate and MCC preparation was performed according to Moya et al [21]. This consisted of drying fresh PALF for 4 weeks in a solar dryer, milling, and sieving it down to a 0.85 mm particle diameter (Mesh 20). Composition of dried PALF in terms of ash, water, lignin, hemicelluloses and alpha-cellulose contents were determined according to corresponding ASTM methods. Dried PALF was treated with 2% NaOH aqueous solution at 80°C for 4 hours, and then bleached with a 2.5% $NaClO_2$ solution at room temperature for another 4 hours to obtain a cellulosic mass. This mass was then refluxed in presence of HCl 2 N at 90°C for 15 minutes, washed with distilled water until pH reached a neutral value, and then treated with 0.25% aqueous ammonia and washed again to obtain a solution with a pH 7 to obtain MCC. Finally, MCC was dried inside an air circulating oven at 80°C for 10 hours. Hereafter, the lignocellulosic starting material will be referred as PALF, the cellulosic mass extracted from PALF substrate will be referred as CELLULOSE, and microcrystalline cellulose will be referred as MCC.

Characterization of the cellulosic materials was performed with a Perkin Elmer Paragon 1000 PC Fourier transform infrared spectrometer (FITR), and wide-angle X-ray scattering (WAXS) in a Bruker DS Advance with CuKα, 2θ scanning between 5° and 40° at 1° per minute. In addition, thermal stability of PALF, CELLULOSE, and MCC was assessed by thermogravimetrical analysis (TGA) in a TA Instruments Q500 TGA, operated from 50° to 800°C at 20 °C/min under inert atmosphere.

2.3 Composites Preparation and Characterization

Three series of PLA composite films were cast from chloroform solutions containing 2 wt. %, 4 wt. %, 6 wt. %, 8 wt. % and 15 wt. % of MCC. The first group labeled as MCC-X (where X stands for MCC weight percentage), contained PLA and MCC dispersed in chloroform as follows: PLA was first dissolved in chloroform at 35°C, MCC was then added and mixed for 5 hours at 700 rpm on a magnetic heater, then cooled down to room temperature, poured into a rectangular glass mold, and kept under vacuum at 40°C for two weeks. A second group, T-MCC-X, contained pretreated MCC fibers with TBA. Treated fibers were prepared by mixing MCC with TBA in a 1:1 ratio on a magnetic heater at 600 rpm and 30°C, then filtered and dried inside an air circulating oven for 3 hours and 70°C. T-MCC was then dispersed into the PLA chloroform solution by following the procedure presented above. A third group of samples labeled as ST-MCC-X also contained TBA-treated MCC particles, in addition to 10 wt. % of PEG 400 surfactant dispersion aid.

Thermal properties of the composite films were analyzed by using a Differential Scanning Calorimeter (DSC) operated over the temperature range of 50-200°C at a heating rate of 10 °C/min under nitrogen gas atmosphere in a Perkin Elmer DSC 6.

Tensile properties of the composites were assessed by an Instron 3365, placing rectangular pieces (50 mm × 10 mm × 0.2 mm) of each film with a gauge length of 20 mm, at 5 mm/min, and using a 1 kN load cell. Dynamic mechanical properties of the composites were evaluated by means of a Perkin Elmer DMA 8000 scanning from room temperature to 150ºC at 2 ºC/min in tension mode, 1 Hz and 0.050 strain. Finally, the state of dispersion was assessed by means of an Olympus BX43 optical microscope with a 4X lens, and a SC30 camera.

3 Results and Discussion

3.1 Characterization of the Cellulosic Materials

Tab. 1 shows the chemical composition of PALF obtained in this work in comparison to those reported in earlier works. Values reported by Quesada [8] and Cordoba [24] were both obtained with local PALF samples according to standard ASTM methods, whereas results reported by Mukherjee and Satyanarayana [25], Mohanty et al. [26], and Mishra et al. [27] were obtained with Indian PALF substrates and no details on test procedures were declared. In addition, values reported by Khalil et al. [28] were obtained with Malaysian PALF substrates using TAPPI methods. In spite of the differences observed in the PALF chemical composition, it was clear that PALF possesses high cellulose content which would be useful in polymer composites.

Table 1: Chemical composition of PALF

Chemical property	**Present work**	**Quesada**	**Córdoba**	**Mukherjee Mohanty Mishra**	**Khalil**
Ashes (wt. %)	4.64	4.60	12.06	1.1	2.0
Humidity (wt. %)	8.90	13.5	8.64	11.8	****
Lignin (wt. %)	25.63	27.72	8.3	5-12	10.5
Hemicellulose (wt. %)	17.43	****	****	****	****
α-Cellulose (wt. %)	45.32	45.12	****	70-82	73.4
Holocellulose (wt. %)	****	42.70	66.2	****	80.5

Lignocellulose, cellulose, and microcrystalline cellulose extracted from PALF were subjected to X-ray scattering, FTIR, and thermal analysis. WAXS diffractograms of PALF, cellulose and MCC (Fig. 1) show three characteristic peaks in a 2θ scan [22,23]; a first peak close to 15° attributed to both (110) and ($1\bar{1}0$) planes; a second peak around 22° due to (200) crystal plane, and a third peak at 35° due to the (004) plane. X-ray pattern for PALF shows the influence of amorphous materials such as lignin and hemicellulose.

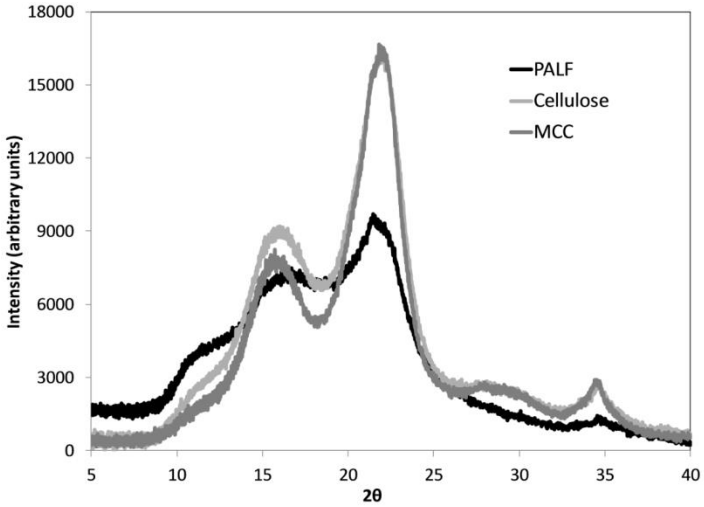

Figure 1: WAXS diffractograms of PALF, cellulose and MCC

Diffraction patterns for both cellulose and MCC were similar to each other. Crystallinity index (*CI*) from X-ray data was determined using the peak intensity height ratio method as described by Park et al [23]. Values of *CI* for PALF, cellulose, and MCC were 35%, 59% and 70%, respectively. These results reflected a significant increase in the extent of the crystalline cellulose due to a more ordered and compact crystal structure in MCC. Published *CI* values for MCC from different agricultural sources other than cotton were in the 60%-70% range [1,3-5], which was in agreement with the *CI* value obtained in this work.

Thermal stability of the cellulosic components was analyzed by means of TGA, and their results are shown in Fig. 2.

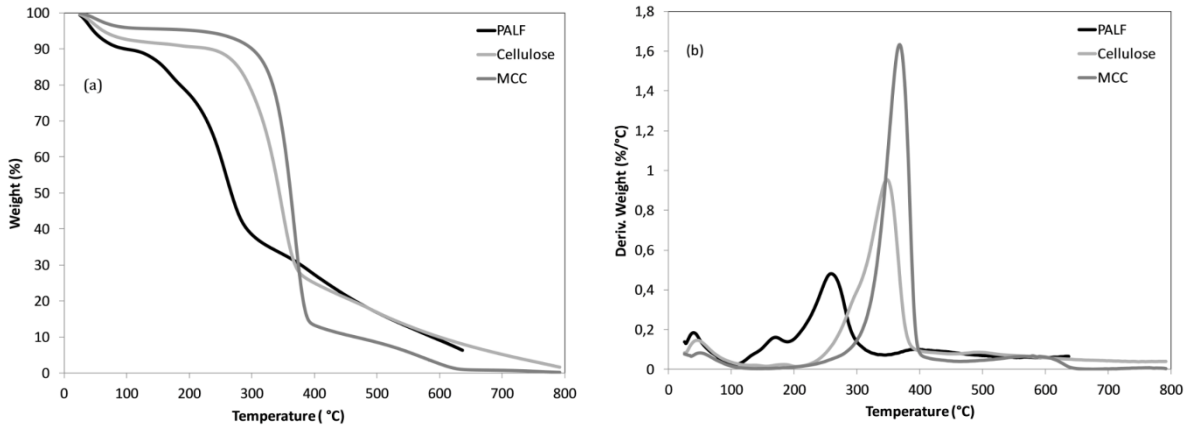

Figure 2: Thermogravimetrical traces (a) and thermogram derivatives (b) of PALF, cellulose and MCC

It is known that thermal behavior of lignocellulosic fibers could be different, depending on the type and the nature of the source [29]. However, agro waste materials usually showed similar trends in the way that they thermally decompose, i.e., water release around 100°C, cellulose decomposition between 210 and 260°C, hemicellulose decomposition from 160°C to 280°C, and finally lignin decomposition starting at 220°C and continuing above 400°C [30-32]. These multiple thermal decomposition events were easily seen in the case of PALF substrate, as it can be observed in Figs. 2(a) and 2(b). Similar thermal behavior for pineapple leaves and stems was reported recently by Zainuddin et al. [33]. On the other hand, a progressive increase in thermal stability could be observed for cellulose and MCC, which can be correlated to the increase of the extent of cellulose crystallinity [1]. There was a reduction in the number

of thermal events in cellulose and MCC, as shown in Fig. 2, as the extraction and hydrolysis treatments removed significant extents of hemicellulose and lignin. As it can be seen in Fig. 2(a), a certain amount of lignin was still present in MCC (around 10 wt. %), as this material usually decomposes over a wider range of temperature than cellulose [34]. Furthermore, lignin fraction in MCC degraded between 400 and 600°C and left almost no char at around 700°C, in contrast to PALF and cellulose (Fig. 2).

FTIR spectra of PALF, cellulose and MCC are presented in Fig. 3, and assigned peaks are presented in Tab. 2. These spectra were significantly similar to each other with some differences worth to be noticed:

- The ratio of peak heights of the peaks located at 3400 cm^{-1} and 2900 cm^{-1} decreased as PALF was converted into MCC, which indicated a more significant presence of aliphatic C-H bonds
- The peak height at around 1650 cm^{-1} which corresponds to conjugated carbonyl groups in lignin [35] decreased as PALF was converted into MCC
- The peak which corresponds to the β-glycosidic linkage [36] at around 900 cm^{-1} was clearly seen as a shoulder both in MCC and cellulose, whereas it was overlapped with the C-O/C-C stretching vibration at 1060-1024 cm^{-1} in PALF spectrum.

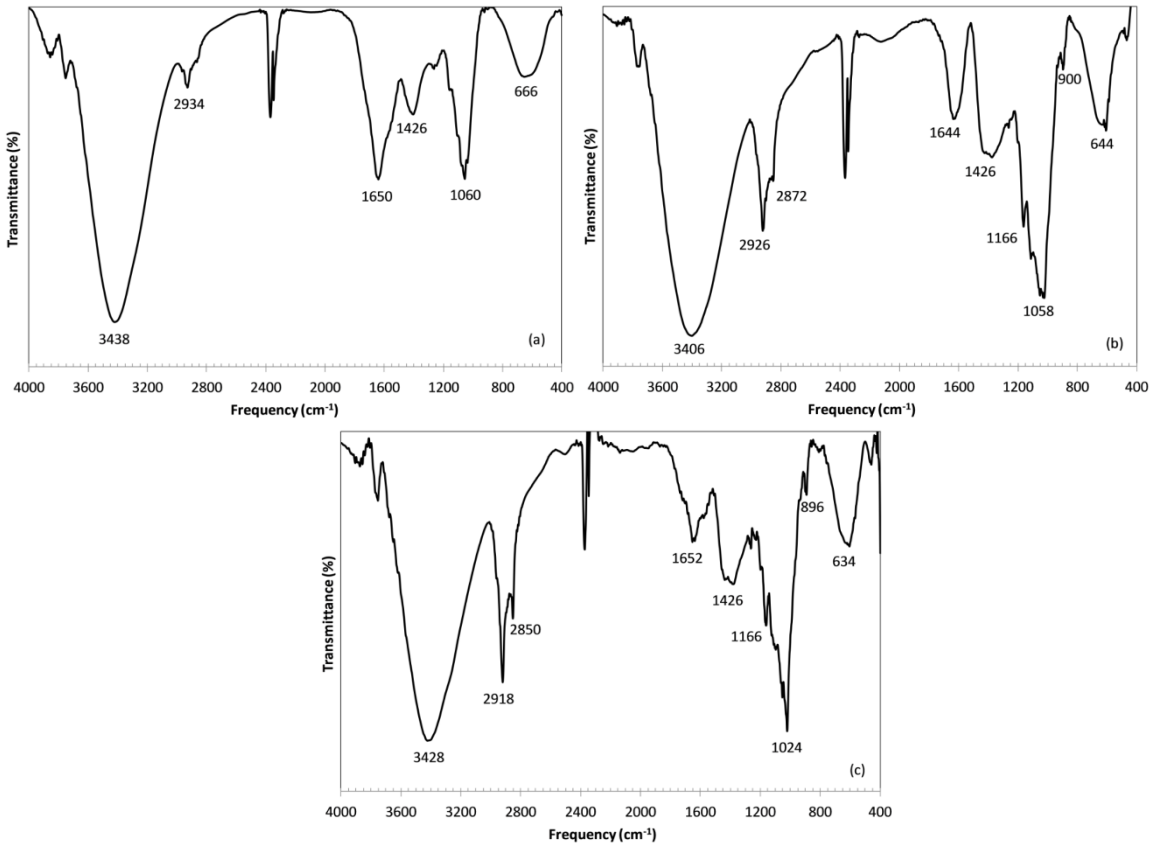

Figure 3: FT-IR spectra of (a) PALF, (b) cellulose and (c) MCC

There are few comprehensive reports concerning on detailed FTIR characterization of PALF and its derivatives. One recent work dealing with the characterization of industrial by-products of pineapple by Ramos et al. [37] reported the presence of type-II crystalline cellulose in pineapple by-products using IR signals between 1336 cm^{-1} and 1314 cm^{-1}. However, such signals could not be detected in this present work. In addition, Ramos et al. [37] correlated signal at 900 cm^{-1} to the presence of amorphous cellulose based on the paper of Ciolacu et al. [38]. These authors assigned the peak at 1430 cm^{-1} to crystalline cellulose based on commercial MCC. Therefore, Ramos et al. [37] referred to the signal at 900 cm^{-1} as the

"amorphous band", and 1430 cm^{-1} as the "crystalline band" in cellulose. In the present work, the amorphous band could be resolved and observed in cellulose and MCC at 900 cm^{-1}.

Table 2: IR frequency assignment (cm^{-1}) for PALF, cellulose and MCC

PALF	Cellulose	MCC	Assignment
3438	3406	3428	O-H stretching
2934	2926-2872	2918-2850	C-H stretching
1650	1644	1652	C=O stretching in lignin
1426	1426	1426	Symmetric CH_2 bending
1160	1166	1166	Asymmetric C-O-C ring
1060	1058	1024	C-O/C-C stretching
***	900	896	β-glycosidic linkage
666	644	634	H-bonded O-H out of plane bending

Meanwhile, the crystalline peak height at 1430 cm^{-1} (in our analysis located at 1426 cm^{-1}) increased in cellulose and MCC samples, as compared to that in PALF sample, in agreement with our TGA and WAXS results.

3.2 Characterization of the Biocomposite Films

Melting behavior of the composites was characterized by DSC as presented in Fig. 4, and the extent of crystallinity of the PLA phase in the composites, (calculated with the assumption of a heat of fusion of 93 J/g for a 100% crystalline PLA [39]), is shown in Fig. 5. Fig. 4(a) shows DSC curves for PLA/MCC composites without any chemical treatment or additive. These curves showed no significant change in their shape and transition temperature values. However the heat of fusion gradually decreased as the MCC content increased. Therefore, PLA crystallinity was drastically reduced as it can be observed in Fig. 5. It is inferred that the extent of interaction between the polymer matrix and MCC was limited, and MCC hindered crystallization of PLA chains. In addition, neither glass transition nor cold crystallization was observed for these composites. Mathew et al. [11] reported a nucleating effect of commercial MCC in PLA after melt extrusion followed by injection molding, and suggested that transcrystallization of PLA occurred at the filler-matrix interface. Nucleation effects were not clearly observed when PLA was solution mixed in the presence of commercial cellulose microfibers by Sanchez et al. [12]. Nevertheless, Sanchez et al. also suggested the presence of transcrystallization.

In the case of PLA/T-MCC composites (Fig. 4(b)) a different thermal behavior was observed. In these composites, transcrystallinity was observed with the appearance of multiple endothermic peaks around the PLA melting temperature at around 150°C. This finding suggests that T-MCC acted as a nucleating agent in PLA crystallization during the film casting, which increased the extent of polymer crystallinity as shown in Fig. 5. PLA multiple fusion endotherms were also observed by Sanchez et al. [12], and nucleating effects of MCC were also reported by Mathew et al. [11]. Recall, however, that both works were based on commercially available MCC samples. Kim et al. [14], also reported multiple PLA melting peaks in the presence of flour from pineapple peel. Fig. 4(c) shows thermal data for ST-MCC composites, and Fig. 5 shows the extent of crystallinity in these samples. It is evident that the presence of PEG reduced the extent of crystallinity in neat and filled PLA samples. A multiple endotherm pattern could be observed during melting of the PLA composites filled with ST-MCC, although this was not as significant as in the case of T-MCC composites. As it was expected, neat PLA crystalline domains were affected by the presence of PEG as shown in Fig. 5.

Furthermore, PLA crystallinity showed an increase only in the presence of 2 wt.% of ST-MCC. It appeared that beyond this filler content, the nucleation effect of TBA-treated MCC was limited by the presence of the surfactant.

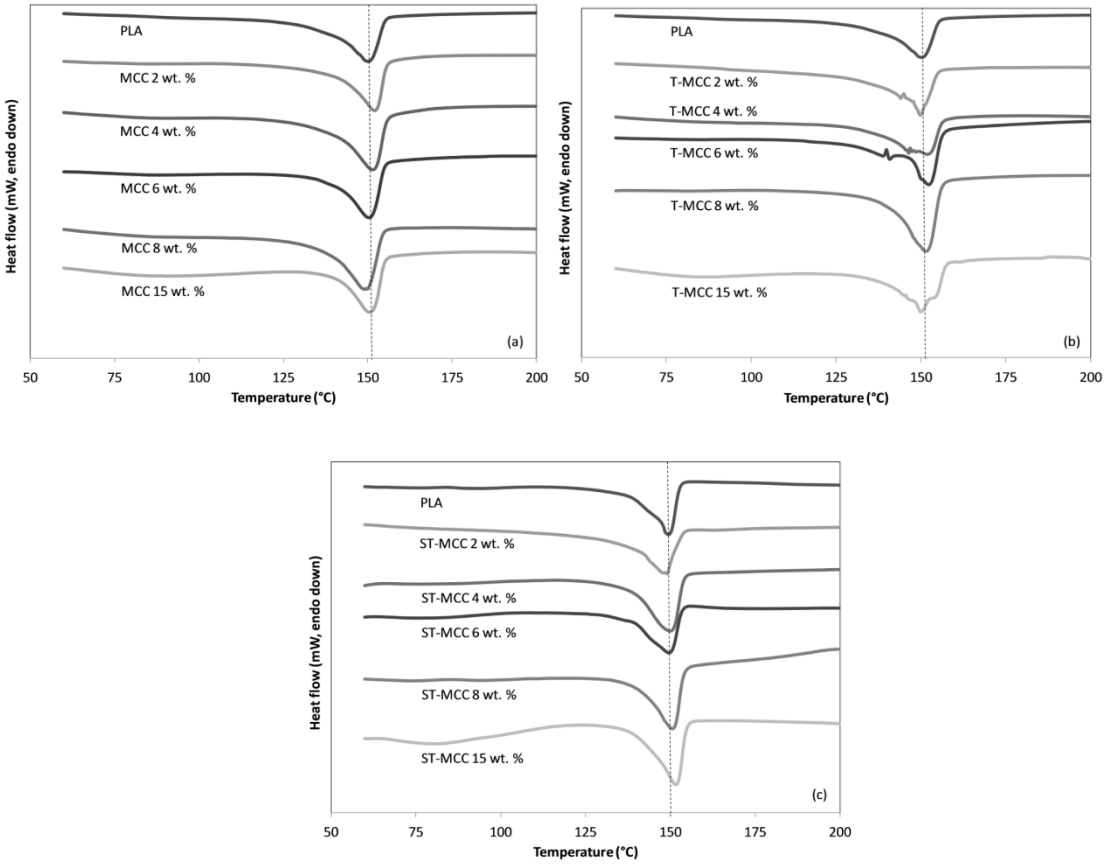

Figure 4: DSC thermograms of (a) PLA/MCC, (b) PLA/T-MCC, and (c) PLA/ST-MCC composites

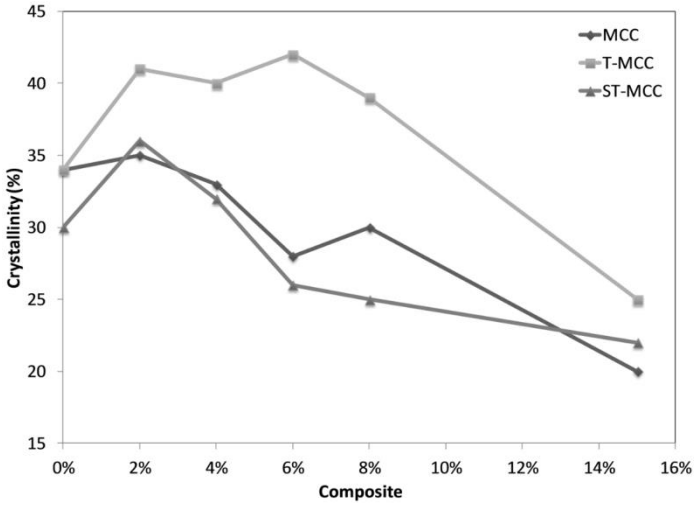

Figure 5: Crystallinity of PLA composites

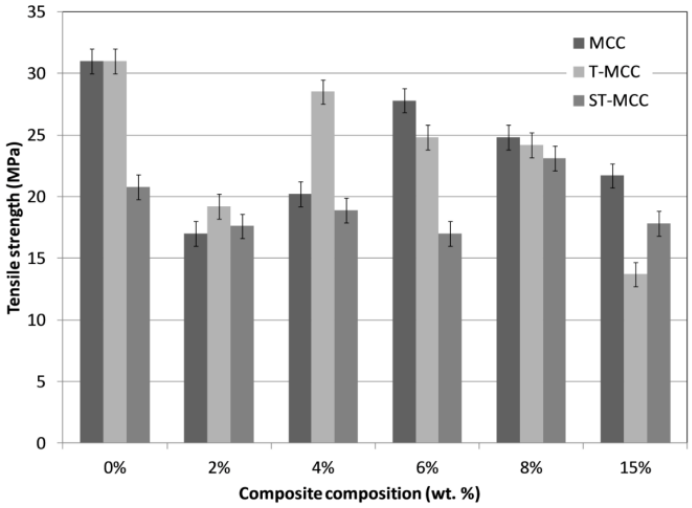

Figure 6: Tensile stress of PLA composites

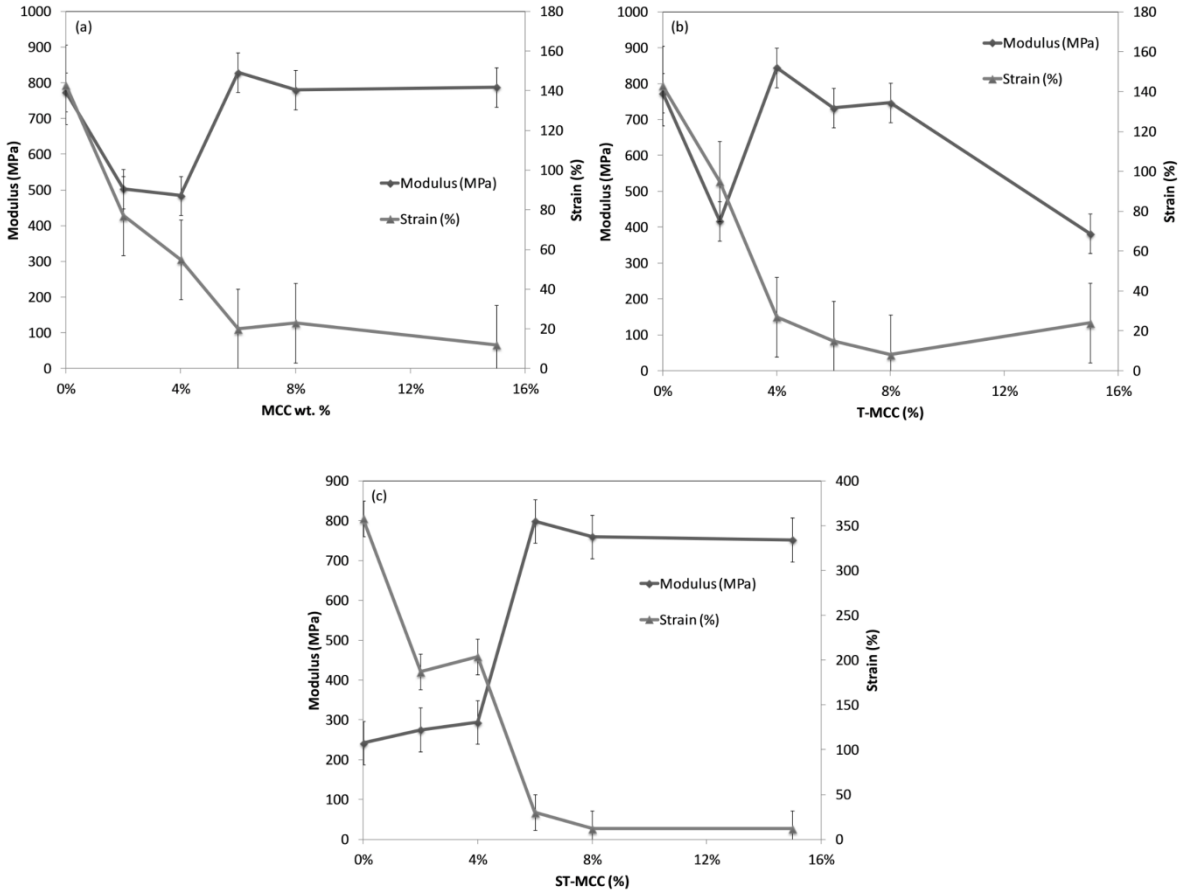

Figure 7: Tensile modulus and strain of (a) PLA/MCC, (b) PLA/T-MCC, and (c) PLA/ST-MCC

Tensile testing data of all three sets of PLA composites are presented in Figs. 6 and 7. As expected, tensile strength values for PLA/MCC, PLA/T-MCC and PLA/ST-MCC composites were lower than that of neat PLA (Fig. 6). Similar trend was reported by Mathew et al. [10], who concluded that lower strength values originated from poor interfacial bonding. In all cases, strain values also decreased in the presence of fillers. On the other hand, tensile modulus slightly increased in the presence of 6 wt. % of MCC and

leveled off (Fig. 7(a)) at higher MCC contents. In T-MCC composites, modulus reached a maximum at 4 wt. %, and dropped in the presence of 15 wt. % of T-MCC (Fig. 7(b)). In addition, ST-MCC composites showed an increase in tensile modulus in the presence of 6 wt. % of the filler, and then leveled off (Fig. 7(c)). In these composites, tensile modulus was affected due to reduction in PLA crystallinity in the presence of PEG. Therefore, the presence of ST-MCC was able to compensate this reduction at a filler content of 6 wt. %. Strain values of PLA in the presence of PEG increased 150% comparing with neat PLA.

Dynamic mechanical properties of the composites were analyzed and shown in Fig. 8. There was a tendency in MCC and T-MCC composites to increase their storage modulus in comparison with neat PLA, especially in the range of 40°C and 80°C.

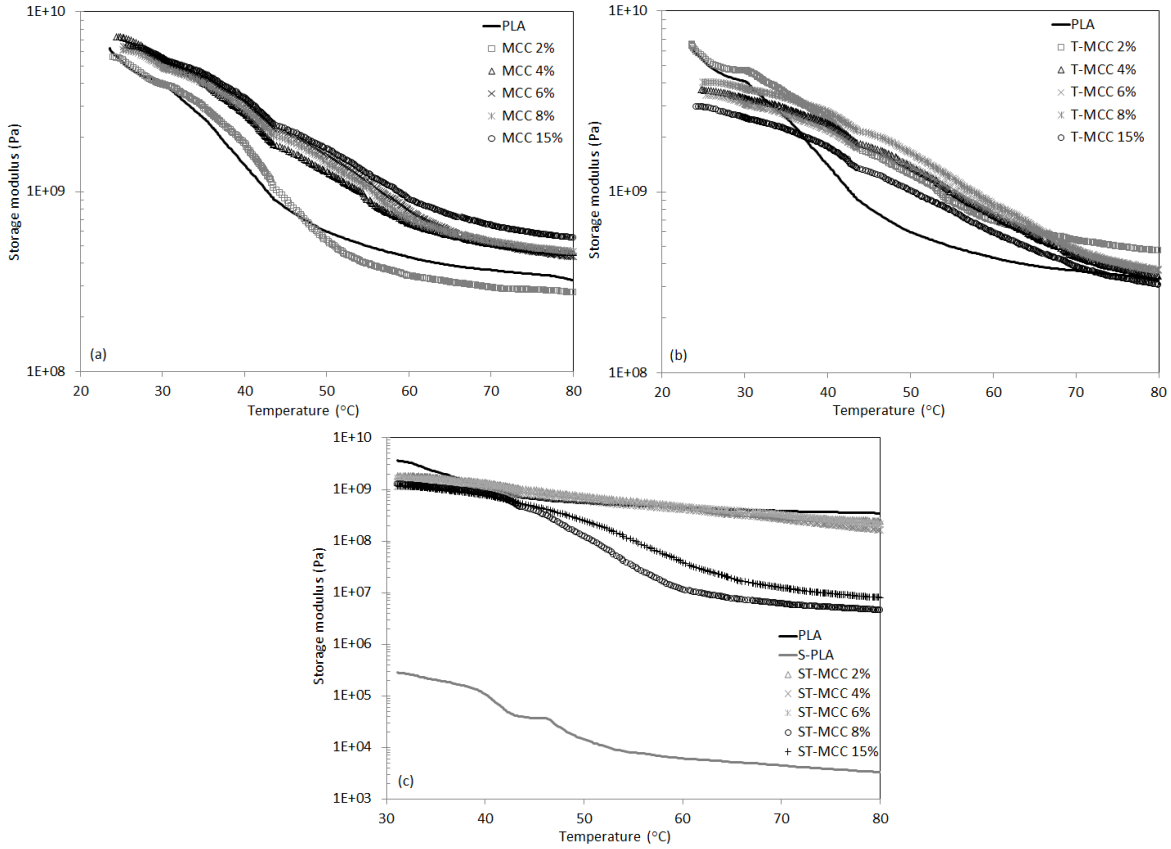

Figure 8: Dynamic modulus of (a) PLA/MCC, (b) PLA/T-MCC, and (c) PLA/ST-MCC

This behavior was also reflected in PLA glass transition measured through tan δ values of neat PLA and its composites (Tab. 3). Glass transition temperature of PLA increased as the microcrystalline cellulose content increased. Both MCC and T-MCC showed good interaction with the amorphous PLA chains, therefore restricting their motion [10]. However, there was a difference in the thermomechanical behavior of PLA when T-MCC is used instead of MCC. Recall that the crystallization behavior of PLA in the presence of T-MCC, and the presence of MCC are different (Fig. 5). DMA results combined with the crystallization data in Fig. 5, suggested that T-MCC interacted with both amorphous and crystalline PLA regions while MCC only interacted with the amorphous PLA chains. Similar findings were obtained by Petersson et al. [40]. These authors combined PLA with cellulose nanowhiskers previously treated with tert-butanol, and observed an improvement on the storage modulus and tan δ peak temperature, when TBA-treated cellulose was used. They attributed it to a better dispersion of the TBA-treated whiskers. On

the other hand, ST-MCC composites showed a completely different behavior. Since these composites contained a surfactant agent, neat PLA containing PEG (S-PLA) was also tested. A dramatic drop in the storage modulus of PLA in the presence of PEG can be seen in Fig. 8(c). Storage modulus of ST-MCC filled PLA samples was similar to that of neat PLA. However, modulus at higher temperature was significantly lower beyond 8 wt. % ST-MCC content, perhaps due to the lower extent of crystallinity in these samples.

Table 3: Temperatures (°C) measured at tan δ for PLA composites

Wt. %	MCC	T-MCC	ST-MCC
0	42	42	52
2	43	47	51
4	46	54	62
6	50	54	59
8	48	54	54
15	51	54	59

Agglomeration of MCC particles was another issue to address. In this work, PEG and TBA were used to enhance the state of MCC dispersion in the polymer matrix. Optical micrographs of composite films with 4 wt. % of MCC, T-MCC and ST-MCC are shown in Fig. 9. All composites showed MCC agglomerates with sizes between 100 μm and 200 μm. However, the presence of PEG helped to reduce the size of the agglomerates.

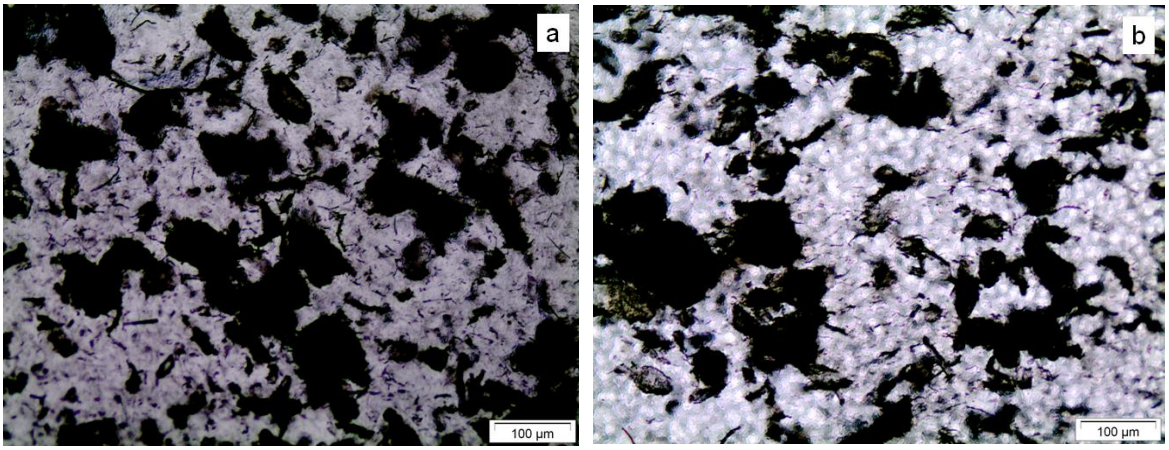

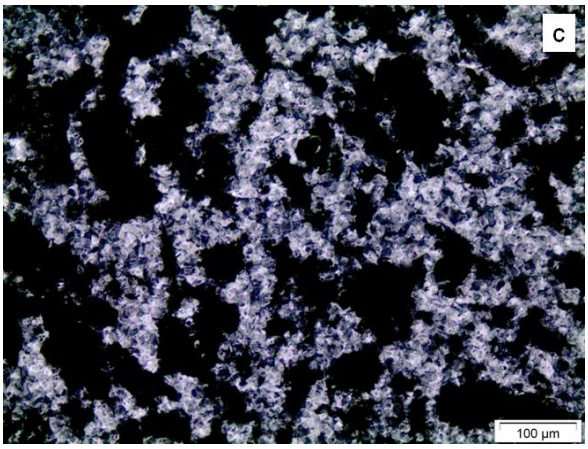

Figure 9: Optical micrographs of PLA and 4 wt. % of (a) MCC, (b) T-MCC and (c) ST-MCC

4 Conclusions

Treatment of MCC with tert-butyl alcohol proved to be useful at improving the crystal nucleation capability of MCC in the PLA matrix. Tensile modulus of the composites increased in the presence of 4 wt. % MCC or higher. The presence of the surfactant agent reduced the extent of crystallinity in PLA matrix which resulted in large strain values, although did not provide major advantages in thermal properties of the composites. A MCC content of 4 wt. % or 6 wt. % appeared to provide balanced engineering properties.

Acknowledgements: This research received grant from the Costa Rican Council of Science and Technology (CONICIT) and the Costa Rican Ministry of Science, Technology and Telecommunications (MICITT). Authors are thankful to the School of Chemistry at the Universidad of Costa Rica for XRD data.

References

1. Azubuike CP, Odulaja JO, Okhamafe AO. Physicotechnical, spectroscopic and thermogravimetric properties of powdered cellulose and microcrystalline cellulose derived from groundnut shells. *Journal of Excipients and Food Chemicals* **2012**, 3: 106-115.
2. Paralikar KM, Bhatawdekar SP. Microcrystalline cellulose from bagasse pulp. *Biological Wastes* 1988, **24**:75-77.
3. Tang LG, Hon DNS, Pan SH, Zhu YQ, Wang Z, Wang ZZ. Evaluation of microcrystalline cellulose. I. Changes in ultrastructural characteristics during preliminary acid hydrolysis. *Journal of Applied Polymer Science* **1996**, 59: 483-488.
4. Eichhorn SJ, Young RJ. The Young´s modulus of a microcrystalline cellulose. *Cellulose* **2001**, 8: 197.
5. Bochek AM, Shevchuk IL, Lavrent'ev VN. Fabrication of microcrystalline and powdered cellulose from short flax fiber and flax straw. *Russian Journal of Applied Chemistry* **2003**, 76: 1679-1682.
6. Uesu NY, Gómez EA, Winkler AA. Microcrystalline cellulose from soybean husk: effects of solvent treatments on its properties as acetylsalicylic acid carrier. *International Journal of Pharmaceutics* **2000**, 206: 85-96.
7. Durán-Chavarría M, Moya-Portuguéz M, Umaña-Rojas E, Jimenez G. Plastification of cellulosic wastes. In J. F. Kennedy, G. O. Phillips, P. A. Williams (Eds.), *Recent Advances in Environmentally Compatible Polymers*. Woodhead, UK. **2001**: 67.
8. Quesada-Solis K, Alvarado-Aguilar P, Sibaja-Ballestero R, Vega-Baudrit J. Utilizacion de las fibras del rastrojo de piña (Ananas comusus, variedad champaka) como material de refuerzo en resinas de polyester. *Revista Iberoamericana de Polímeros* **2005**, 6(2).
9. Satyanarayana KG, Arizaga GC, Wypych F. Biodegradable composites based on lignocellulosic fibers-an overview. *Progress in Polymer Science* **2009**, 34: 982-1021.

10. Mathew AP, Oksman K, Sain M. Mechanical properties of biodegradable composites from poly lactic acid (PLA) and microcrystalline cellulose (MCC). *Journal of Applied Polymer Science* **2005**, 97: 2014.
11. Mathew AP, Oksman K, Sain M. The effect of morphology and chemical characteristics of cellulose reinforcements on the crystallinity of polylactic acid. *Journal of Applied Polymer Science* **2006**, 101: 300-310.
12. Sanchez-Garcia MD, Gimenez E, Lagaron JM. Morphology and barrier properties of solvent cast composites of thermoplastic biopolymers and purified cellulosic fibers. *Carbohydrate Polymers* **2008**, 71: 235-244.
13. Mukherjee T, Kao N, Gupta RK, Quazi N, Bhattacharya SN. Reinforcing function of surface acetylated cellulose on polylactic acid (PLA) based biopolymer. *Proceedings of the 36th Annual Condensed Matter and Materials Meeting* **2012**: 1-4
14. Kim KW, Lee BH, Kim HJ, Sriroth K, Dorgan JR. Thermal and mechanical properties of cassava and pineapple flours-filled PLA bio-composites. *Journal of Thermal Analysis and Calorimetry* **2012**, 108().
15. Mukherjee T, Kao N. PLA based biopolymer reinforced with natural fibre: a review. *Journal of Polymers and the Environment* **2011**, 19: 714.
16. Nampoothiri KM, Nair NR, John RP. An overview of the recent developments in polylactide (PLA) research. *Bioresource Technology* **2010**, 101: 8493-8501.
17. Haafiz MKM, Hassan A, Zakaria Z, Inuwa IM, Islam MS, Jawaid M. Properties of polylactic acid composites reinforced with oil palm biomass microcrystalline cellulose. *Carbohydrate Polymers* **2013**, 98: 139-145.
18. Oksman K, Mathew AP, Bondeson D, Kvien I. Manufacturing process of cellulose whiskers/polylactic acid nanocomposites. *Composite Science and Technology* **2006**, 66: 2776-2784.
19. Halász K, Csóka L, Rákosa R. Application of nano and micro sized cellulose crystals in poly(lactic Acid). *Proceedings of the International Scientific Conference on Sustainable Development and Ecological Footprint* **2012**.
20. Dos Santos FA, Tavares MIB. Preparing films from poly(lactic acid) and microcrystalline cellulose and characterization. *Polímeros* **2013**, 23: 229.
21. Moya M, Sibaja M, Pereira R, Nikolaeva S, Vega-Baudrit J. Síntesis y Caracterización de Celulosa Microcristalina (CM) de Materiales Naturales. *Proceedings of the 12th International Congress of Engineering* **2000**.
22. Thygesen A, Oddershede J, Lilholt H, Thomsen AB, Ståhl K. On the determination of crystallinity and cellulose content in plant fibres. *Cellulose* **2005**, 12: 563.
23. Park S, Baker JO, Himmel ME, Parilla PA, Johnson DK. Cellulose crystallinity index: measurement techniques and their impact on interpreting cellulose performance. *Biotechnology for Biofuels* **2010**, 3: 10.
24. Córdoba M. Determinación del Efecto de la Concentración de la Base NaOH, de la Celulosa y la Celobiasa en la Hidrólisis para la Producción de Etanol a partir de Rastrojo de Piña (Ph.D. Thesis). Universidad de Costa Rica. **2011**.
25. Mukherjee PS, Satyanarayana KG. Structure and properties of some vegetable fibres. *Journal of Materials Science* **1986**, 21: 51.
26. Mohanty AK, Misra M, Hinrichsen G. Biofibres, biodegradable polymers and biocomposites: an overview. *Macromolelcular Materials and Engineering* **2000**, 276/277: 1.
27. Mishra S, Mohanty AK, Drzal LT, Misra M, Hinrichsen G. A review on pineapple leaf fibers, sisal fibers and their composites. *Macromolelcular Materials and Engineering* **2004**, 289: 955.
28. Khalil HPSA, Alwani MS, Omar AKM. Chemical composition, anatomy, lignin distribution, and cell wall structure of Malaysian plant waste fibers. *BioResources* **2006**, 1(2): 220.
29. Ogah AO, Afiukwa JN, Englund K. Characterization and comparison of thermal stability of agro waste fibers in bio-composites application. *Journal of Chemical Engineering and Chemistry Research* **2014**, 1: 84.
30. Saheb DN, Jog JP. Natural fiber polymer composites: a review. *Advances in Polymer Technology* **1999**, 18: 351.
31. Monteiro SN, Calado V, Margem FM, Rodriguez RJS. Thermogravimetric stability behavior of less common lignocellulosic fibers-a review. *Journal of Materials Research and Technology* **2012**, 1(3): 189-199.
32. Monteiro SN, Calado V, Rodriguez RJS, Margem FM. Thermogravimetric behavior of natural fibers reinforced polymer composites-an overview. *Materials Science and Engineering A* **2012**, 557: 17-28.
33. Zainuddin MF, Shamsudin R, Mokhtar MN, Ismail D. Physicochemical properties of pineapple plant waste fibers from the leaves and stems of different varieties. *BioResources* **2014**, 9(3): 5311.
34. Brebu M, Vasile C. Thermal degradation of lignin-a review. *Cellulose Chemistry and Technology* **2010**, 44: 353.

35. Sim SF, Mohamed M, Lu NALMI, Sarman NSP, Samsudin SN. Computer-assisted analysis of Fourier transform infrared (FTIR) spectra for characterization of various treated and untreated agriculture biomass. *BioResources* **2012**, 7(4): 5367.
36. Samal RK, Ray MC. Effect of chemical modifications on FTIR spectra. II. Physicochemical behavior of pineapple leaf fiber (PALF). *Journal of Applied Polymer Science* **1997**, 64: 2119-2125.
37. Ramos ME, Sanchez ME, Rojas M, Mora R. Structural, physicochemical and functional properties of industrial residues of pineapple. *Cellulose Chemistry and Technology* **2014**, 48: 633.
38. Ciolacu D, Ciolacu F, Popa VI. Amorphous cellulose-Structure and characterization. *Cellulose Chemistry and Technology* **2011**, 45: 13-21.
39. Fischer EW, Sterzel HJ, Wegner G. Investigation of the structure of solution grown crystals of lactide copolymers by means of chemical reactions. *Kolloid Zeitschrift und Zeitschrift für Polymere* **1973**, 251: 980-990.
40. Petersson L, Kvien I, Oksman K. Structure and thermal properties of poly(lactic acid)/cellulose whiskers nanocomposite materials. *Composite Science and Technology* **2007**, 67: 2535-2544.